# An Imaging Protocol to Discriminate Specialized Conduction Tissue During Congenital Heart Surgery

*Abhijit Mondal, PhD,[*,1] John Lackey, MS,[†,1] Mossab Saeed, MD,[*] Fei-Yi Wu, MD,[¶] Jordan K. Johnson, BS,[†,‡] Chao Huang, PhD,[‡,§] Frank B. Sachse, PhD,[†,‡] Robert Hitchcock, PhD,[†] and Aditya K. Kaza, MD[*,†]*

We performed preclinical validation of intraoperative fiber-optic confocal microscopy (FCM) and assessed its safety and efficacy in an ovine model of the pediatric heart. Intraoperative imaging was performed using an FCM system (Cellvizio, Mauna Kea Technology, Paris, France) with specialized imaging miniprobe (GastroFlex UHD, Mauna Kea Technologies). Before imaging, we applied an extracellular fluorophore, sodium fluorescein, to fluorescently label extracellular space. We imaged arrested hearts of ovine (1–6 months) under cardiopulmonary bypass. Image sequences (1–10 seconds duration) were acquired from regions of the sinoatrial and atrioventricular node, as well as subepicardial and subendocardial working myocardium from atria and ventricle. The surgical process was evaluated for integration of the imaging protocol during the operative procedure. In addition, fluorescein cardiotoxicity studies ($n = 3$ animals) were conducted by comparing electrocardiogram (PR and QRS intervals) and ejection fraction at baseline and after topical application of fluorescein at 1:10, 1:100, and 1:1000 dilutions on a beating ovine heart. Our studies suggest that intraoperative FCM can be used to identify regions associated with specialized conducting tissue in ovine hearts in situ. The imaging protocol was integrated with conventional open heart surgical procedures with minimal changes to the operative process. Application of fluorescein in varying concentrations did not affect the normalized PR interval, QRS interval, and ejection fraction. These preclinical validation studies demonstrated both safety and efficacy of the proposed intraoperative imaging approach. The studies constitute an important step toward first-in-human clinical trials.

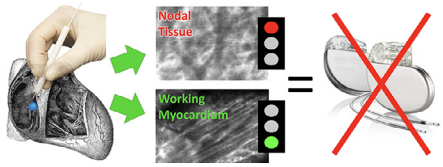


Utilization of confocal microscopy can help with tissue discrimination inside the heart.

**Central Message**

Fiber-optics confocal microscopy (FCM) can be used intraoperatively to visualize and identify specialized conduction tissues.

**Perspective Statement**

A significant barrier in pediatric reconstructive heart surgery is the accurate intraoperative localization of conducting tissues in patients with complex congenital heart disease. Damage to these tissues can lead to sinus node dysfunction and atrioventricular block. Here, we validate the safety and efficacy of intraoperative fiber-optics confocal microscopy in an ovine model of the pediatric heart.

**Semin Thoracic Surg 31:537–546** © 2019 Elsevier Inc. All rights reserved.

**Keywords:** Translation, Preclinical, Tissue imaging, Conductive tissue, Validation

*Abbreviations:* ACT, activated clotting time; AV, atrioventricular; ECG, electrocardiogram; FCM, fiber-optics confocal microscopy; FDA, Food and Drug Administration; IVC, inferior vena cava; OR, operating room; SA, sinoatrial; SVC, superior vena cava

*Department of Cardiac Surgery, Boston Children's Hospital, Boston, Massachusetts
†Department of Biomedical Engineering, University of Utah, Salt Lake City, Utah
‡Nora Eccles Harrison Cardiovascular Research and Training Institute, University of Utah, Salt Lake City, Utah
§Comprehensive Arrhythmia and Research Management (CARMA) Center, University of Utah, Salt Lake City, Utah
¶Division of Cardiovascular Surgery, Department of Surgery, Taipei Veterans General Hospital, Taipei City, Taiwan

Funding: This work was supported by the National Institutes of Health (R56 HL128813 and R01 HL135077).

Conflicts of Interest: The authors Huang, Sachse, Hitchcock, and Kaza have been granted patents and applied for patents associated with the techniques described in this paper.

[1]John Lackey and Abhijit Mondal contributed equally to this manuscript.

Address reprint requests to Aditya Kaza, MD, Department of Cardiac Surgery, Boston Children's Hospital and Harvard Medical School, 300 Longwood Ave, Bader 273, Boston, MA 02115. Robert Hitchcock, PhD, Department of Biomedical Engineering, University of Utah, 36 S Wasatch Drive, 4509 SMBB, Salt Lake City, UT 84112.

## INTRODUCTION

The disposition of the cardiac conduction system in the normal heart is well documented by morphologic studies.[1] Accurate intraoperative localization of specialized conducting tissue in a pediatric population of congenitally deformed hearts presents a unique challenge. In congenitally deformed hearts, the disposition of these vital structures cannot be accurately identified, and the surgeon must approximate the location of these anatomical sites.[2,3] If these tissues are damaged during surgical repair, the cardiac conduction system can be disrupted and the patient may experience temporary or permanent heart block.[4–6] Table 1 lists the incidence rates of conduction abnormalities after surgical repair of ventricular septal defects,[5,7] atrioventricular canal defects,[5,6,8] tetralogy of Fallot,[4,6,8] sinus venosus atrial septal defects,[9–11] and transposition of the great arteries.[12,13] Conduction abnormalities such as dysfunction of sinoatrial (SA) and atrioventricular (AV) conduction pathways require chronic cardiac rhythm management using permanent pacemaker implantation, creating a high economic and societal burden.[14,15]

Fiber-optics confocal microscopy (FCM) was developed as an alternative to traditional biopsies used in standard endoscopic evaluations. The technology produces optical sections, allowing clinicians to evaluate tissue microstructure at the point of care through real time in vivo visualization at depths of up to 100 μm below the tissue surface. Fiber-optic imaging systems have been approved for clinical use in urogenital,[16] gastrointestinal,[17] and pulmonary[18] applications. In our previous studies, we introduced approaches based on FCM and extracellular fluorophore delivery for imaging of the living heart.[19–21] These approaches allowed us to identify atrial working myocardium and tissue regions associated with the conduction system based on microstructural arrangements in these tissue types. We hypothesize that surgeons can use these approaches to more accurately localize specialized conducting tissue and prevent injury to these vital tissues during surgical repair. Identifying specific tissue types during surgery may reduce postsurgical complications resulting from trauma to the cardiac conduction system.[6] Though the imaging system and dye delivery methods were suitable for use in a rodent model, validation protocols are required to demonstrate safety and efficacy for clinical use.[22]

The aim of this study was to evaluate our previously developed approaches in the operative setting. Our research group has been moving toward clinical translation with rodent studies,[21] ex vivo human studies,[20] expert human analysis,[22] and here with preclinical validation studies for safety and efficacy. This approach takes advantage of an US Food and Drug Administration (FDA)-approved imaging system in an off-label application that may have a profound effect on the comorbidities associated with pediatric congenital heart surgery. In this paper, we describe the steps that we took to perform preclinical validation and obtain regulatory approval prior to performing first-in-human studies.

## METHODS

### Sheep Anesthesia and Surgical Protocol

The experimental studies were IACUC approved and conducted at the Animal Resources at Children's Hospital (ARCH) facility (Boston, MA). An experimental ovine animal was induced with Ketamine (Fort Dodge Animal Health, Overland Park, KS) at a dose of 10 mg/kg IV and Midazolam (Hospira, Lake Forest, IL) at a dose of 0.2–0.5 mg/kg IV and maintained with 1–4% isoflurane (Patterson Veterinary Supplies Inc., Devens, MA) with intubation and mechanical ventilation. Blood from a donor animal was used for priming the cardiopulmonary bypass circuit and for transfusions to replace blood loss during surgery. The experimental ovine was placed in supine position and sternotomy was performed. Bicaval cannulation was setup with 14–18 Fr cannula (Medtronic, Minneapolis, MN). The right femoral artery was then cannulated with 8–12 Fr cannula (Medtronic, Minneapolis, MN) based on the size of the animal. The animal was systemically heparinized (300 units/kg) (Fresenius Kabi, Canton, MA) and the cardiopulmonary bypass was started once activated clotting time was >720 seconds. The heart was arrested using del Nido cardioplegia solution (20 mL/kg) (Central Admixture Pharmacy Services, Inc., Woburn, MA) delivered via the aortic root after cross-clamp application. The superior vena cava and inferior

**Table 1.** Incidence Rate of Conduction Abnormalities and Permanent Pacemaker Implantation After Surgical Repair of Various Congenital Heart Defects Leading to Sinoatrial and Atrioventricular Conduction Abnormalities

| Congenital Defect | Conduction Abnormality Type | Conduction Abnormality % | Permanent Pacemaker Implantation % |
|---|---|---|---|
| Ventricular septal defects (VSD) | | | |
| Perimembranous VSD | Atrioventricular | – | 1.1[7] |
| Atrial switch with VSD | Atrioventricular | – | 6.5[5] |
| Arterial switch with VSD | Atrioventricular | – | 3.4[5] |
| Coarctation with VSD | Atrioventricular | – | 1.7[5] |
| Atrioventricular canal defect | Atrioventricular | – | 1–2.3[5,6,8] |
| Tetralogy of Fallot | Atrioventricular | 3[4] | 0.9–1.4[6,8] |
| Sinus venosus atrial septal defect | Sinoatrial | 6–35[9–11] | 4.6[10] |
| Transposition of the great arteries | Sinoatrial | 11–64[12,13] | 3.8–7.5[12,13] |

vena cava were snared for total bypass. FCM imaging was first done at the SA node region and the working myocardium. Right atriotomy was performed for imaging the AV node region. After imaging, 6-0 Prolene marking sutures (Ethicon Inc., Somerville, NJ) were placed on the FCM imaged sites in the SA and AV node regions. The right atrium was closed using 5-0 Prolene (Ethicon Inc., New Jersey, USA) and the animal was taken off bypass. After the heart regained normal beating for approximately 10 minutes, the animal was euthanized by intravenous administration of Fatal Plus (Vortech Pharmaceuticals Ltd., Dearborn, MI).

### FCM Imaging and OR Integration

FCM imaging was conducted on arrested hearts of 1−6-month-old ovine on cardiopulmonary bypass. Sodium fluorescein (Fluorescite 10%, Alcon Laboratories Inc., Fort Worth, TX) was delivered either topically (animals: 16) or systemically via cardioplegia (animals: 6). For topical application, 100 mg/mL fluorescein was diluted 1:1000 in saline. The dilute solution was applied via syringe at a volume of 1−2 mL on the tissue surface 2−3 seconds before imaging. For systemic dye delivery, 100 mg/mL fluorescein was diluted 1:1000 in cardioplegia and delivered by the catheter inserted in the aortic root perfusing the entire heart via the coronary arteries. The Cellvizio 100 series system (Mauna Kea Technologies, Paris, France) with GastroFlex UHD miniprobe was used for imaging. The system consists of (1) a movable tower that houses the laser scanning unit, control-computer and display, and (2) detachable fiber-optics imaging probes. The tower was placed in the animal OR on the opposite side from the surgeon. The foot pedal was connected and placed by the surgeon's side. A sterile GastroFlex UHD miniprobe with a tip diameter of 2.6 mm was positioned by hand for imaging on the outer heart surface or using forceps inside the heart. Probes were used for up to 20 procedures with reprocessing after each procedure per the manufacturer's instructions. The calibration step was performed automatically by the system once the probe was attached into the laser source. The laser source was controlled directly by the surgeon using the foot pedal or by an assistant using the keyboard. The probe acquired image sequences at a frame rate of 9 Hz with a lateral (*xy* directions) resolution of 1.8 μm, field of view diameter of 240 μm, and at a depth of 55−65 μm from the probe lens-tip. FCM imaging was performed in regions of the SA and AV node, as well as working myocardium of the atria and ventricle. The additional time required for the dye delivery and imaging was recorded.

### Conventional Confocal Microscopy

After euthanasia of the animals, the heart was excised and fixed via antegrade perfusion with a syringe and immersion in Tyrode-like solution containing 4% paraformaldehyde. Immunofluorescent labeling was performed on working myocardium and nodal tissue regions. Dissected tissues were labeled with anti-hyperpolarization-activated cyclic nucleotide-gated potassium channel 4 (HCN4) antibody (Alomone, APC-052, Jerusalem, Israel) and an antibody conjugated to Alexa Fluor 633 (Thermo Fisher, A-21070, Waltham, MA), wheat germ agglutinin (WGA) conjugated with Alexa Fluor 488 (Thermo Fisher, W11261, Waltham, MA), and 4′,6-diamidino-2-phenylindole, dihydrochloride (DAPI) (Thermo Fisher, D1306, Waltham, MA). Three-dimensional imaging of working myocardium and nodal regions was performed using a scanning confocal microscope (TCS SP8, Leica Microsystems, Wetzlar, Germany). Imaged regions included the endocardial face of right ventricular working myocardium and the endocardial face of the AV nodal regions adjacent to the suture marker.

### Assessment of Acute Fluorescein Cardiotoxicity

Fluorescein is an FDA-approved dye commonly administered intravenously and utilized for ophthalmic vascular imaging. Acute cardiotoxicity of fluorescein was evaluated by applying different concentrations of fluorescein on the beating ovine heart in situ. Four solutions were prepared using saline and 100 mg/mL fluorescein. Saline was used for baseline recordings. The remaining 3 solutions were 1:1000 (0.1 mg/mL), 1:100 (1 mg/mL), and 1:10 (10 mg/mL) dilutions of stock fluorescein dye in saline. Three animals 1−6 months old and weighed 10−35 kg were selected for the study. A median sternotomy was performed on anesthetized animals followed by incision of the pericardium to access the heart. From lowest to highest fluorescein concentration, each solution was sequentially dispensed via syringe at a volume of 5 mL on the beating heart surface. The solutions were dispensed in a manner to ensure uniformity and complete coverage of the heart surface. Immediately following topical application of each solution, echocardiographic imaging of the left ventricle and electrocardiogram (ECG) recordings were performed for 5−10 minutes. Echocardiographic imaging was done using a diagnostic ultrasound system (Model iE33, Philips, Andover, MA). ECGs were recorded using a Cardio Companion esophageal electrode system (SurgiVet, Smiths Medical, Norwell, MA). ECG signals were acquired and printed using Advisor Vital Signs Monitor (SurgiVet, Smiths Medical, Norwell, MA). The P wave and QRS complex were identified in the ECG strips. The PR and QRS intervals were measured for 5 beats from the ECG strips for each condition for each animal. Ejection fractions were calculated using the analysis software of the diagnostic ultrasound system. Left ventricular areas during diastole and systole were manually identified and marked on the echocardiographs for the analysis.

### Expert Analysis

FCM videos of 1−10 seconds duration were acquired during surgery and indexed based on anatomical origin, that is, working myocardium or nodal. Shorter 1−2 seconds video clips were generated and randomly selected for evaluation by examiners blinded to the tissue type. Video clips were incorporated into a graphical user interface (MATLAB 2017b) that played the video and prompted examiners for classification.

Prior to classification, examiners were trained using a slide presentation consisting of previously indexed still images and

video clips that illustrated microstructural features indicative of each tissue type. Examiners reviewed the set of video clips of working myocardium and nodal tissue and asked to classify each video as either working myocardium or nodal tissue. We defined true positive and true negative outcomes as working myocardium correctly classified as working myocardium and nodal tissue correct classified as nodal tissue, respectively. Sensitivity and specificity of the examiners in discriminating working myocardium and nodal tissue in video clips were determined according to these classifications.

### Sample Sizes and Statistics

Fluorescein cardiotoxicity testing was performed with 3 animals. The test protocols were developed in consultation with the FDA as part of the Investigational New Drug (IND) application. The PR intervals, QRS intervals, and ejection fractions for each animal were normalized to their respective mean baseline by the following equation:

$$X_{\text{norm}} = \frac{X_{\text{condition}}}{\overline{X}_{\text{baseline}}} \quad (1)$$

where $X_{\text{norm}}$ was the normalized value of the selected parameter $X$, $X_{\text{condition}}$ was the recorded parameter value, and $\overline{X}_{\text{baseline}}$ was the mean of the recorded values at baseline condition for the respective animal. Normalized ejection fraction values were calculated in percentage, where Eq. (1) was multiplied by 100. For FCM expert analysis study, an a priori power analysis (G*Power 3.1.9.2, University of Duesseldorf) was performed.[23] A minimum sample size of 81 per group was estimated to achieve statistical power of 0.8 and detect an effect across the 2 groups with medium effect size of 0.4 and significance criteria of 0.05.

## RESULTS

### FCM Imaging and OR Integration

A total of 22 female juvenile sheep (age: 0.9—7.7 months, weight: 11.1—37 kg) were used for FCM imaging using either topical ($n = 16$) or systemic ($n = 6$) application of fluorescein. Imaging in atrial and ventricular regions showed regular striated tissue microstructures while those in the SA and AV node regions displayed irregular and reticulated microstructures (Fig. 1; Videos 1—6 in Supplementary Material). Similar microstructural features of nodal and non-nodal regions were present in our previous studies with heart tissues from rodent, neonatal lamb, and humans using FCM.[20—22] Figure 2 shows example images from 3D conventional confocal microscopy of a nodal region and a working myocardium region. Both

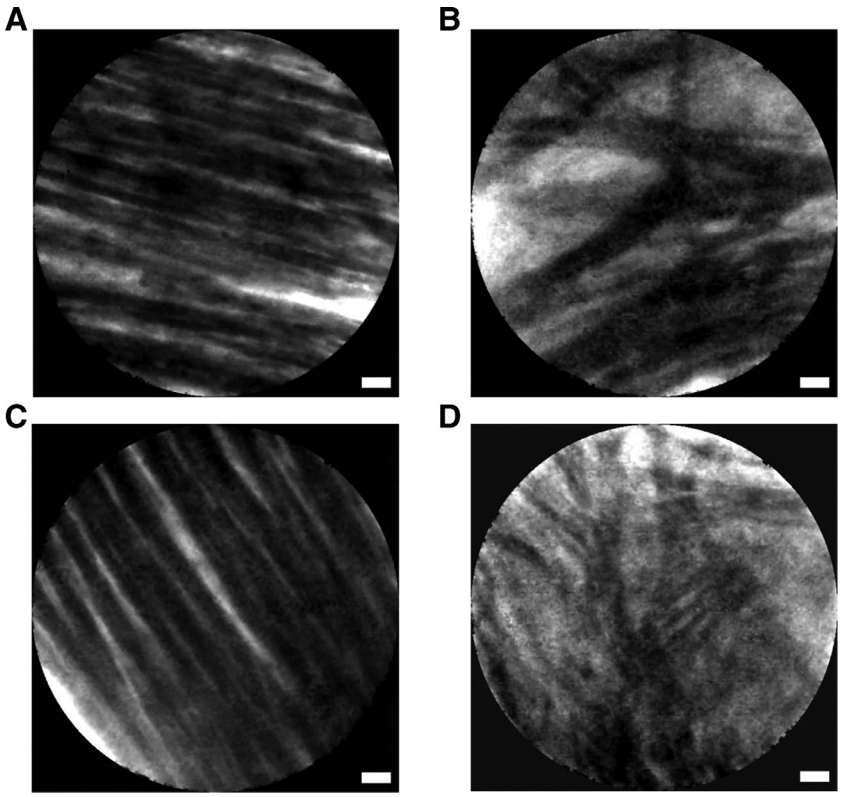


**Figure 1.** Video frames from FCM of living arrested ovine heart. Images were acquired by the surgeon using the imaging probe after topical administration of 1:1000 dilution of fluorescein for visualization of working myocardium (A, C) and nodal region (B, D). Fluorescein remains in the extracellular space and allows visualization of the cell boundaries to highlight the tissue microstructure. The working myocardium (A, C) presents striated tissue microstructure compared to reticulated microstructure in nodal regions (B, D). Scale: 20 μm.

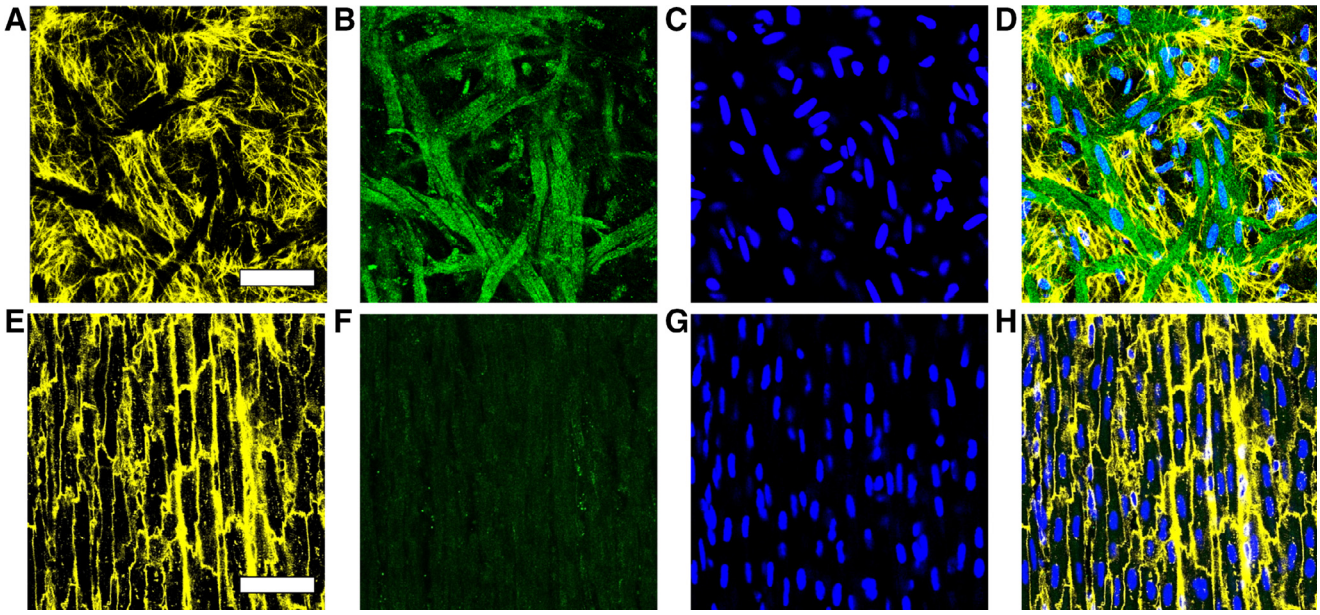


**Figure 2.** Confocal images of immunohistochemically labeled tissue from an atrioventricular node region (A–D) and working myocardium (E–H). Tissues were fluorescently labeled with WGA in yellow (A, E), HCN4 in green (B, F) and DAPI in blue (C, G). WGA identifies the extracellular space. HCN4 is a marker of nodal and pacemaker cells, but not of working myocardium. DAPI marks cell nuclei. (D) and (H) are composite images showing the labels. Note that HCN4 labeled positive only for cells in the nodal region (B) that presented a reticulated tissue microstructure (A) in contrast to the working myocardium that was HCN4 negative (F) and has a striated tissue microstructure (E). Scale: 50 μm. (Color version of figure is available online.)

regions stained positive for WGA and DAPI. In contrast to the working myocardium, WGA images from the nodal region exhibited reticulations and are positive for HCN4.

A distinct difference in contrast was observed during FCM imaging of the SA node region between the 2 dye delivery methods. Images from topical dye delivery revealed clearly distinguishable tissue microstructure in all regions of the heart. In contrast, images from systemic dye delivery displayed inferior contrast with indistinguishable tissue microstructure in the SA node region.

The addition of the movable tower, foot pedal, and probe into the animal OR was viewed favorably by the surgical team. The surgeon spent 4.9 ± 0.7 seconds ($n = 4$) to load the syringe with dye and apply 2–3 mL of fluorescein and 1.9 ± 1.1 seconds ($n = 7$) to place the syringe back on the instrument table. Direct administration of dye via the cardioplegia solution did not add to the procedure time. It took the surgeon 2.3 ± 0.6 seconds ($n = 7$) to pick up the FCM probe for imaging and 2.7 ± 0.7 seconds ($n = 3$) to place it down after imaging. FCM video clips of 1–10 seconds durations were acquired during imaging.

## Assessment of Acute Fluorescein Cardiotoxicity

Table 2 summarizes the electrocardiographic and echocardiographic values and parameters of sheep from literature[24–30] and those recorded in our studies. The electrocardiographic and echocardiographic parameters vary with breed, age, and geographic location, as well as from animal to animal. The recorded parameters from the 3 animals were normalized to their respective mean baseline values in each animal to account for variations observed in the animals used in the study. The normalized ejection fractions for the different fluorescein dilutions are presented in Figure 3A. There were no clinically meaningful differences in mean normalized ejection fraction following application of each dye dilution condition.

Similarly, for the ECG data, PR and QRS intervals for different fluorescein dilutions were normalized to baseline recordings. The mean normalized intervals for all 3 fluorescein dilutions were close to baseline (Supplementary Figs. 1–4) suggesting that fluorescein application has no effect on cardiac conduction. The normalized results are presented in Figure 3B.

## Expert Analysis

A random set of video clips of 81 working myocardium and 81 nodal regions were evaluated by 8 examiners blinded to the tissue type. Examiners evaluated the images after being trained to identify characteristic features in the microstructural arrangement of each tissue type. The examiners achieved a high sensitivity and specificity of 93.5 ± 3.6% and 96.8 ± 3.9%, respectively (Table 3). Examiners incorrectly classified approximately 5 working myocardium videos as nodal tissue (false negative) and approximately 3 nodal region videos as working myocardium (false positive) out of the total 162 videos.

**Table 2.** Electrocardiographic and Echocardiographic Parameters of Ovine Models

| | Electrocardiogram | | Echocardiogram |
|---|---|---|---|
| | PR Interval (s) | QRS Complex (s) | Ejection Fraction % |
| Literature | 0.045 ± 0.008[24]<br>0.077 ± 0.015[25]<br>0.105 ± 0.019[26]<br>0.180 ± 0.016[27] | 0.095 ± 0.005[24]<br>0.042 ± 0.009[25]<br>0.057 ± 0.013[26]<br>0.060 ± 0.010[27] | 59.4 ± 4.9[28]<br>51.4 ± 12.9[29]<br>41.2 ± 6.7[30] |
| Dye study: Baseline | 0.190 ± 0.033 | 0.074 ± 0.010 | 69.3 ± 11.0 |
| Dye study: 1:1000 dilution | 0.185 ± 0.077 | 0.077 ± 0.019 | 66.0 ± 7.8 |
| Dye study: 1:100 dilution | 0.175 ± 0.033 | 0.076 ± 0.013 | 69.7 ± 9.0 |
| Dye study: 1:10 dilution | 0.190 ± 0.030 | 0.075 ± 0.018 | 71.0 ± 10.7 |

## DISCUSSION

We did not observe any complications resulting from the cardiac bypass procedures used in this study during surgery or FCM imaging. Direct systemic administration of fluorescein did not add any time to the total procedure time. However, systemic administration of fluorescein produced weak contrast in the SA node region. We did not observe this in our previous studies with small animals.[20] Topical dye delivery resulted in superior contrast compared to systemic dye delivery, though it added a short dye application time. While topical dye delivery added ~7 seconds per application, the net time added to the procedure was <40 seconds (~2 mL dye applied each time up to a total of 10 mL). There was an additional probe handling time of <30 seconds (5× probe handling time). Furthermore, systemic administration of dye delivered more dye to the heart than topical application. In systemic application, fluorescein was delivered to the whole heart and ranged from 20 mg to 70 mg based on the amount of cardioplegia infused. In topical application, up to 10 mL of 1:1000 diluted fluorescein was applied, delivering less than 1 mg of fluorescein to the heart. In both cases, the delivered fluorescein was within the tested and reported range of nontoxicity. Operationally, systemic delivery did allow continuous imaging and eliminated handling of the fluorescein-loaded syringe. As neither dye delivery method significantly augmented procedure time and delivered fluorescein was within nontoxic limits, image quality was the primary factor in selecting the preferred dye delivery method. High imaging contrast was vital for effective identification of nodal and non-nodal regions. Hence, topical dye delivery was the superior method.

Possible adverse reactions to fluorescein included vasoplegia, allergic reaction, extravasation, and local tissue damage.[31–33] With the exception of vasoplegia, the listed reactions would have caused ventricular dysfunction measurable by reduction in ejection fraction. We did not observe any significant deviations in ejection fraction from baseline on application of fluorescein dilutions ranging from 1:10 to 1:1000 (Fig. 2). Furthermore, no significant differences were observed in the ECGs recorded before and after application of different fluorescein dilutions (Fig. 3). Our results indicate fluorescein to be noncardiotoxic and safe to use on the heart.

The OR is a demanding environment. During complex pediatric cardiac cases, surgical team members are focused on their individual areas of expertise and are required to communicate as needed to ensure the best patient outcome possible. Introduction of another piece of equipment into this environment requires careful consideration. With the addition of each piece of equipment, the OR becomes more crowded and less efficient, and potential hazards multiply. The imaging system was positioned to minimize interference with the overall procedure (Supplementary Fig. 5). We found that the imaging probes were easy to handle and the imaging screen could be placed out of the way and still be easily visualized by the surgeon. The coordination of imaging probe placement and visualization of the screen was performed without difficulty. Future versions of the probe may include a finger switch similar to a Bovie pen for capturing images. Our results indicate that the equipment can be integrated into the OR with few challenges. However, we note that these studies were performed in an animal OR and the same results may not be found in the human OR.

The laser of the Cellvizio 100 system emits at a wavelength of 488 nm with a maximum power of 15 mW. This was deemed to be a negligible risk as it was approximately 80% less than the maximum allowable retinal exposure as per the standard IEC 60825-1.[34] Thus, we suggest that the fluorescein-based FCM system is a safe intraoperative cardiac imaging modality.

Evaluation of FCM video clips by human examiners indicates that samples from atrial, ventricular, and nodal regions can be distinguished with high sensitivity and specificity. We previously showed that human examiners were able to achieve a higher sensitivity and specificity when reviewing still images from a rodent model in a laboratory environment.[22] Compared to still images, video clips appeared to have a relatively higher level of noise. Motion, film formation or debris, and image artifacts all contributed to a higher level of noise. In addition, some clips did not focus on the tissue region of interest the entire video, leading to possible misclassification.

A technical limitation of the applied FCM system and GastroFlex UHD miniprobe is that imaging was limited to

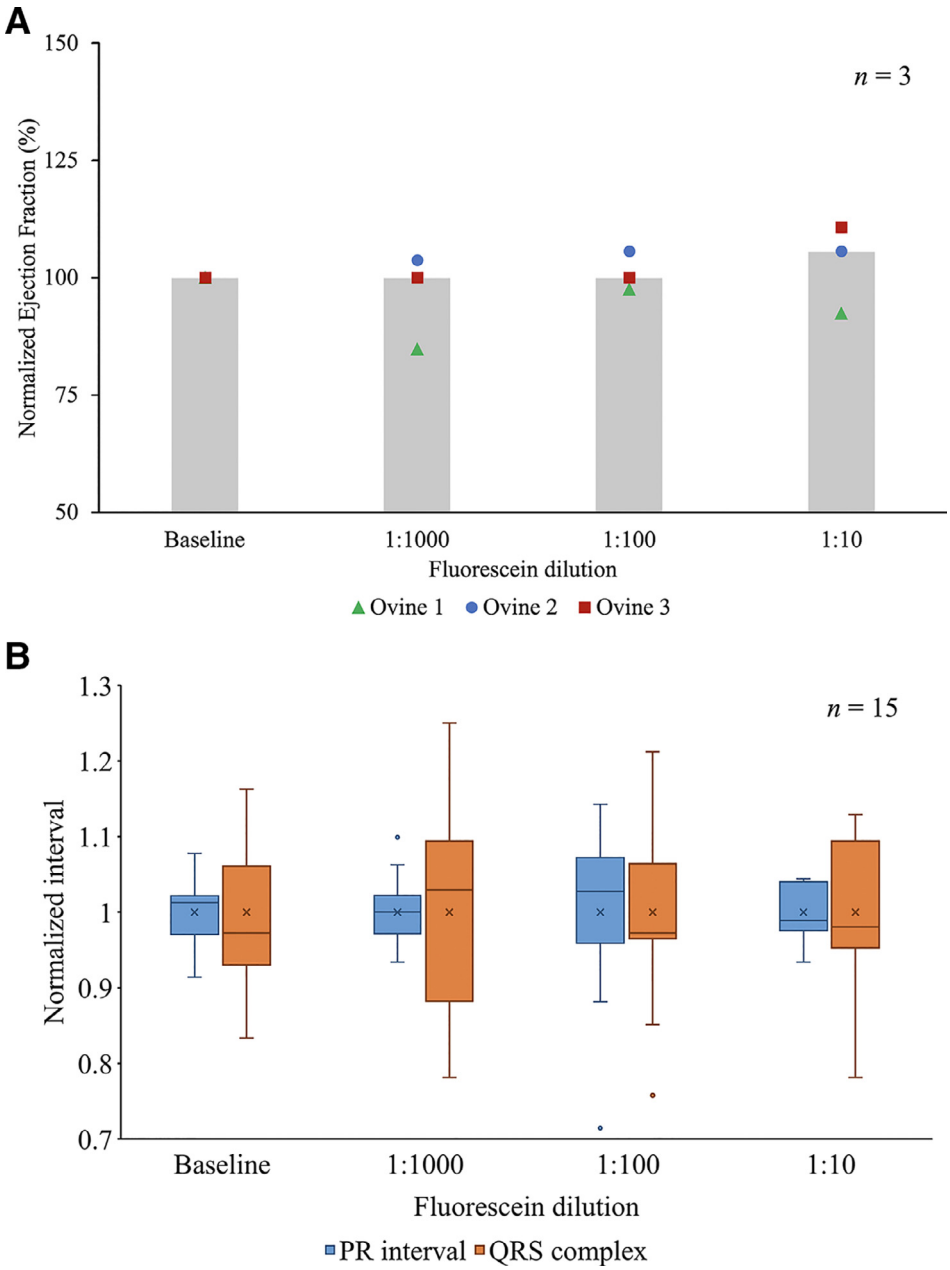


**Figure 3.** Fluorescein cardiotoxicity study results. (A) Normalized ejection fraction vs fluorescein dilution. Ejection fractions were normalized to respective mean baseline values (saline solution). The plot presents the values (dots) and the median (bars) of the normalized ejection fraction in 3 animals ($n = 3$). The effect of fluorescein dilution on normalized ejection fraction appeared to be insignificant. (B) Box and whisker plots of the normalized PR (in blue) and QRS complex (in orange) intervals vs fluorescein dilution. The time intervals were normalized to respective mean interval baseline values (saline). The horizontal line within the box indicates the median, boundaries of the box indicate the 25th and 75th percentile, and the whiskers indicate the maximum and minimum values of nonoutliers. The "x" marked in the box indicates the mean. The extra dots are the outliers. The presented values are from 15 beats ($n = 15$) recorded from 3 animals (5 beats per animal). The effect of fluorescein dilution on normalized PR and QRS complex intervals appeared to be insignificant. (Color version of figure is available online.)

a tissue depth of 55–65 μm. Probes with increased working distance have been developed. However, FCM imaging will not reach tissues at a depth larger than approximately 150 μm and cannot cover the full thickness of the SA or AV node in larger mammals. Thus, the presented images (Fig. 1) present either superficial regions of the nodes or node-associated structures. In our prior work using conventional confocal microscopy in rodents, we showed that surficial tissues with an irregular and reticulated microstructure label positive for HCN4, which is an established

**Table 3.** Examiner Tissue Classification

| Examiner # | Specificity % | Sensitivity % |
|---|---|---|
| 1 | 100.0 | 96.3 |
| 2 | 96.3 | 97.5 |
| 3 | 98.8 | 91.4 |
| 4 | 93.8 | 96.3 |
| 5 | 100.0 | 90.1 |
| 6 | 96.3 | 92.6 |
| 7 | 100.0 | 87.7 |
| 8 | 88.9 | 96.3 |
| Mean ± SD | 93.5 ± 3.6 | 96.8 ± 3.9 |

marker for nodal tissue. A similar finding was presented here for ovine cardiac tissue from a region presumed to be nodal during FCM imaging (Fig. 2).

An operational limitation was the requirement for the surgeon to operate the FCM system and record FCM videos. With the current system setup, the surgeon had to position and hold the probe perpendicular to the tissue surface of the subject while looking at the Cellvizio display in front. This required the surgeon to acclimatize as he/she had to intermittently turn to look down at the subject and forward at the Cellvizio display. A possible solution is to provide a remote monitor located near the subject. Probe maneuverability was challenging in deeper tissue regions, for example AV node and His bundle regions, and forceps had to be utilized to maintain the position and orientation. Furthermore, we note that our ground truth for human expert analysis was based on expertise of the surgeon in identifying nodal regions. In our prior work using a rodent model, we established that an irregular and reticulated microstructure corresponds to nodal tissues using molecular markers.[20]

## CONCLUSION

We performed a preclinical validation of an FCM system on ovine hearts in situ, demonstrating safety and effectiveness of the imaging protocol. The FCM system was successfully integrated into an animal OR suite. Imaging did not add a significant amount of time to the procedure. Expert examiners achieved high sensitivity and specificity discriminating between working myocardium and tissue from nodal regions. The results of this study provide support for advancing to first-in-man studies using real-time FCM for the intraoperative discrimination of cardiac tissue to reduce the incidence of conduction disturbances during surgical repair of congenital heart disease.

## SUPPLEMENTARY MATERIAL

The following is the supplementary data to this article:

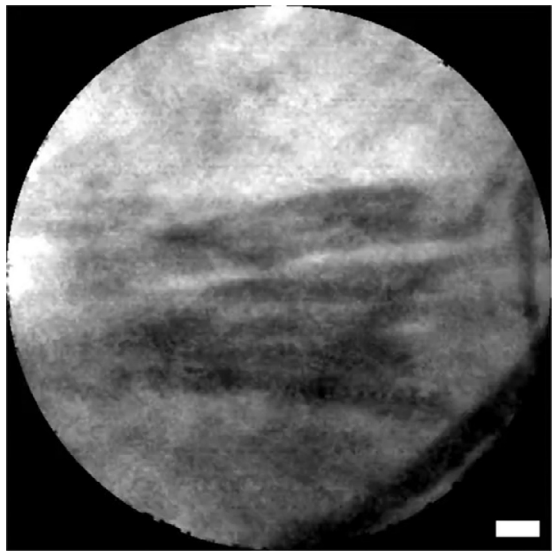

**Video 1.** FCM clip of atrioventricular node region in a cardioplegia arrested ovine heart acquired by the surgeon using the imaging probe after topical application of 1:1000 dilution of fluorescein.

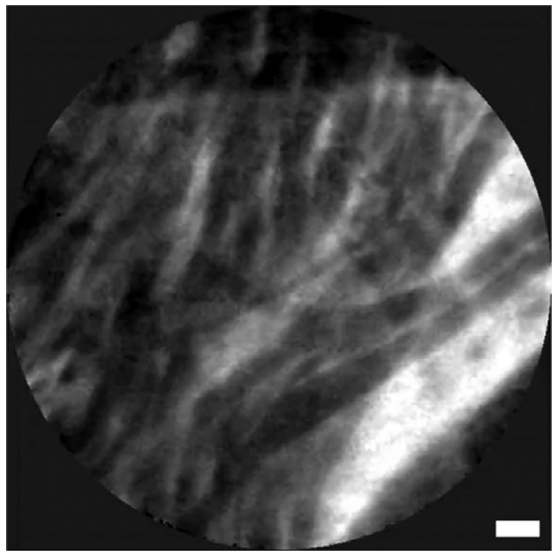

**Video 2.** FCM clip of His bundle region in a cardioplegia arrested ovine heart acquired by the surgeon using the imaging probe after topical application of 1:1000 dilution of fluorescein.

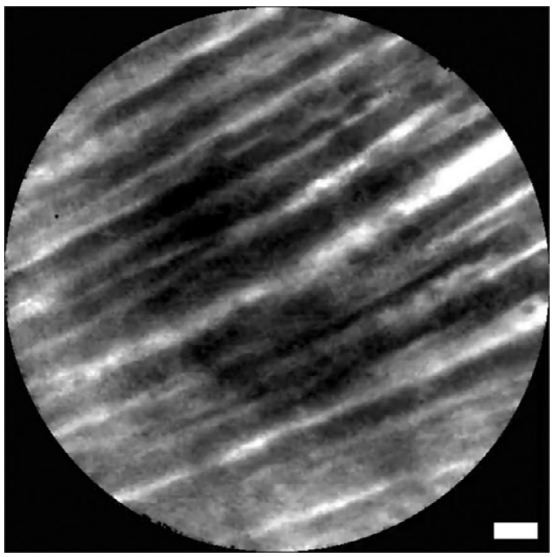

**Video 3.** FCM clip of left ventricular region in a cardioplegia arrested ovine heart acquired by the surgeon using the imaging probe after topical application of 1:1000 dilution of fluorescein.

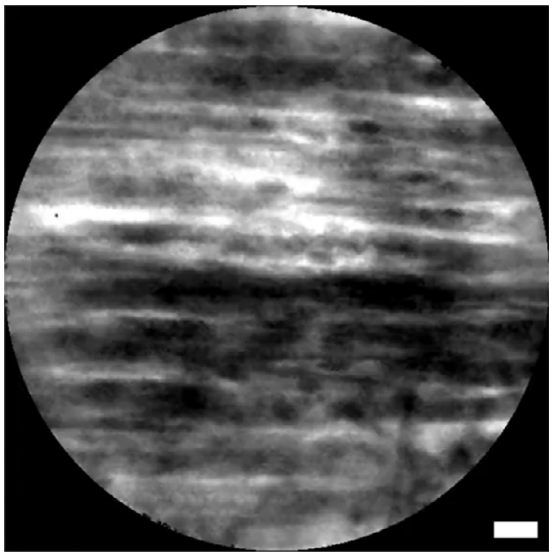

**Video 5.** FCM clip of right ventricular region in a cardioplegia arrested ovine heart acquired by the surgeon using the imaging probe after topical application of 1:1000 dilution of fluorescein.

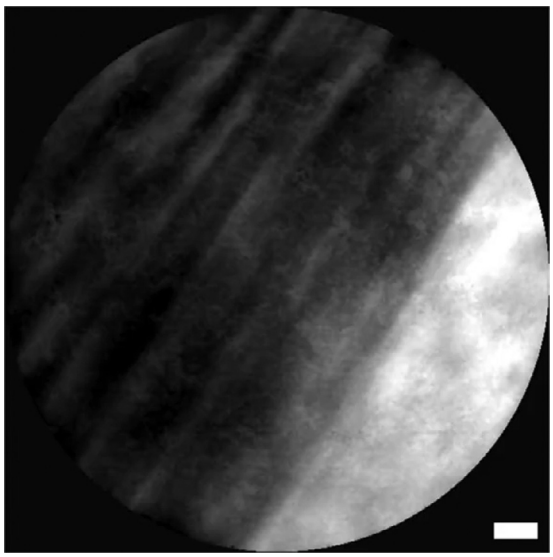

**Video 4.** FCM clip of right atrial region in a cardioplegia arrested ovine heart acquired by the surgeon using the imaging probe after topical application of 1:1000 dilution of fluorescein.

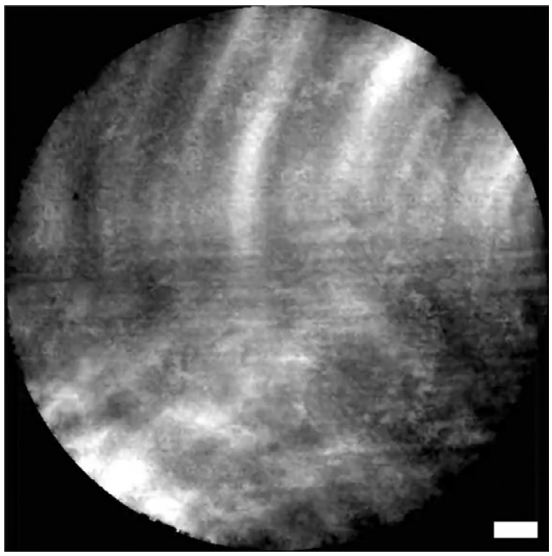

**Video 6.** FCM clip of sinoatrial node region in a cardioplegia arrested ovine heart acquired by the surgeon using the imaging probe after topical application of 1:1000 dilution of fluorescein.

**Video 7.** Dr Kaza providing commentary on preclinical validation of fiber-optic confocal microscopy for congenital heart surgery.

## REFERENCES


1. Allen H, Shaddy R, Penny D, et al: Heart Disease in Infants, Children, and Adolescents: Including the Fetus and Young Adult. p 201, ed 9 Philadelphia: Wolters Kluwer; 2016. p. 201–204
2. Wilcox B, Cook A, Anderson R: Surgical Anatomy of the Heart, 3. New York: Cambridge University Press; 2005. p. 1–328
3. Dick M, Norwood W, Chipman C, et al: Intraoperative recording of specialized atrioventricular conduction tissue electrograms in 47 patients. Circulation 59:150–160, 1979
4. Weindling S, Saul J, Gamble W, et al: Duration of complete atrioventricular block after congenital heart disease surgery. Am J Cardiol 82:525–527, 1998
5. Liberman L, Silver E, Chai P, et al: Incidence and characteristics of heart block after heart surgery in pediatric patients: A multicenter study. J Thorac Cardiovasc Surg 152:197–202, 2016
6. Lin A, Mahle W, Frias P, et al: Early and delayed atrioventricular conduction block after routine surgery for congenital heart disease. J Thorac Cardiovasc Surg 140:158–160, 2010
7. Tucker E, Pyles L, Bass J, et al: Permanent pacemaker for atrioventricular conduction block after operative repair of perimembranous ventricular septal defect. J Am Coll Cardiol 50:1196–1200, 2007
8. Anderson J, Czosek R, Knilans T, et al: Postoperative heart block in children with common forms of congenital heart disease: Results from the KID database. J Cardiovasc Electrophysiol 23:1349–1354, 2012
9. Pace Napoleone C, Mariucci E, Angeli E, et al: Sinus node dysfunction after partial anomalous pulmonary venous connection repair. J Thorac Cardiovasc Surg 147:1594–1598, 2014
10. Jost C, Connolly H, Danielson G, et al: Sinus venosus atrial septal defect: Long-term postoperative outcome for 115 patients. Circulation 112:1953–1958, 2005
11. Stewart R, Bailliard F, Kelle A, et al: Evolving surgical strategy for sinus venosus atrial septal defect: Effect on sinus node function and late venous obstruction. Ann Thorac Surg 84:1651–1655, 2007
12. Gelatt M, Hamilton R, McCrindle B, et al: Arrhythmia and mortality after the mustard procedure: A 30-year single-center experience. J Am Coll Cardiol 29:194–201, 1997
13. Khairy P, Landzberg M, Lambert J, et al: Long-term outcomes after the atrial switch for surgical correction of transposition: A meta-analysis comparing the mustard and senning procedures. Cardiol Young 14:284–292, 2004
14. Weindling S, Saul J, Gamble W, et al: Duration of complete atrioventricular block after congenital heart disease surgery. Am J Cardiol 82:525–527, 1998
15. Silka M, Bar-Cohen Y: A contemporary assessment of the risk for sudden cardiac death in patients with congenital heart disease. Pediatr Cardiol 33:452–460, 2012
16. Wu K, Liu J, Adams W, et al: Dynamic real-time microscopy of the urinary tract using confocal laser endomicroscopy. Urology 78:225–231, 2011
17. Sharma P, Meining A, Coron E, et al: Real-time increased detection of neoplastic tissue in Barrett's esophagus with probe-based confocal laser endomicroscopy: Final results of an international multicenter, prospective, randomized, controlled trial. Gastrointest Endosc 74:465–472, 2011
18. Thiberville L, Saiaiin M, Lachkar S, et al: Human in vivo fluorescence microimaging of the alveolar ducts and sacs during bronchoscopy. Eur Respir J 33:974–985, 2009
19. Lasher R, Hitchcock R, Sachse F: Towards modeling of cardiac microstructure with catheter-based confocal microscopy: A novel approach for dye delivery and tissue characterization. IEEE Trans Med Imaging 28:1156–1164, 2009
20. Huang C, Kaza A, Hitchcock R, et al: Identification of nodal tissue in the living heart using rapid scanning fiber-optics confocal microscopy and extracellular fluorophores. Circ Cardiovasc Imaging 6:739–746, 2013
21. Huang C, Kaza A, Hitchcock R, et al: Local delivery of fluorescent dye for fiber-optics confocal microscopy of the living heart. Front Physiol 5:1–10, 2014
22. Huang C, Sachse F, Hitchcock R, et al: Sensitivity and specificity of cardiac tissue discrimination using fiber-optics confocal microscopy. PLoS One 11:1–13, 2016
23. Faul F, Erdfelder E, Lang A, et al: G*Power 3: A flexible statistical power analysis program for the social, behavioral, and biomedical sciences. Behav Res Methods 39:175–191, 2007
24. Chalmeh A, Saadat Akhtar I, Zarei M, et al: Electrocardiographic indices of clinically healthy Chios sheep. Vet Sci Dev 5:99–102, 2015
25. Koether K, Ulian C, Lourenço M, et al: The normal electrocardiograms in the conscious newborn lambs in neonatal period and its progression. BMC Physiol 16:1, 2015
26. Tajik T, Razavizadeh A, Aslani M, et al: Electrocardiographic parameters in clinically healthy Balouchi sheep. Iran J Vet Sci Technol 7:84–91, 2015
27. Sanyal S, Ahmed J: Electrocardiographic studies in garol sheep and black engal goats. Res J Cardiol 1:1–8, 2008
28. Ikeda Y, Yutani C, Huang Y, et al: Histological remodeling in an ovine heart failure model resembles human ischemic cardiomyopathy. Cardiovasc Pathol 10:19–27, 2001
29. Ghanta R, Rangaraj A, Umakanthan R, et al: Adjustable, physiological ventricular restraint improves left ventricular mechanics and reduces dilatation in an ovine model of chronic heart failure. Circulation 115:1201–1210, 2007
30. Moainie S, Gorman J, Guy T, et al: An ovine model of postinfarction dilated cardiomyopathy. Ann Thorac Surg 74:753–760, 2002
31. Wallace M, Meining A, Canto M, et al: The safety of intravenous fluorescein for confocal laser endomicroscopy in the gastrointestinal tract. Aliment Pharmacol Ther 31:548–552, 2010
32. Yannuzzi L, Rohrer K, Tindel L, et al: Fluorescein angiography complication survey. Ophthalmology 93:611–617, 1986
33. Lopez-Saez M, Ordoqui E, Tornero P, et al: Fluorescein-induced allergic reaction. Ann Allergy Asthma Immunol 81:428–430, 1998
34. International Electrotechnical Commission. Safety of Laser Products: Part 1—Equipment Classification and Requirements. 2014; IEC 60825-1